Explanation of the Different Reaction Behaviors of Bridged and Unbridged Cationic Single Component Zirconocene Catalysts in MMA Polymerizations: a Density Functional Study

Markus Hölscher, Helmut Keul, and Hartwig Höcker*

Lehrstuhl für Textilchemie und Makromolekulare Chemie der RWTH Aachen, Worringer Weg 1, 52074 Aachen, Germany

Received March 18, 2002; Revised Manuscript Received July 29, 2002

ABSTRACT: Density functional (DFT) calculations were carried out on the B3LYP level of theory on bridged and unbridged cationic zirconocene complexes to clarify why unbridged $[Zr(Cp)_2(Me)(thf)][BPh_4]$ is not active in the polymerization of methyl methacrylate (MMA), whereas $[Zr\{(Cp)_2CMe_2\}(Me)(thf)][BPh_4]$ polymerizes MMA readily, as we showed experimentally. It is shown, that the initial step of the polymerization—the transfer of the metallocene bound methyl group to the first MMA molecule—is endothermic for $[Zr(Cp)_2(Me)(MMA)]^+$ but exothermic for $[Zr\{(Cp)_2CMe_2\}(Me)(MMA)]^+$. Furthermore—and more important—the activation energy is higher for the reaction of the unbridged compound compared to the activation energy of the bridged compound. From these results and an estimation of the rate constants it follows that in the temperature range investigated experimentally (−30 to +30 °C) either the endothermic product is not formed at all and/or the reversed reaction to the reactant is much faster than the reaction with the next MMA molecule. These results are confirmed by the inclusion of solvent effects by the CPCM solvation model (also known as COSMO). Alternative reaction paths for both cations were also investigated and found to be energetically much less favorable.

Introduction

The polymerization of methyl methacrylate (MMA) by cationic zirconocenes was first discovered by Collins et al. in 1992,[1] and since then, this field has attracted much interest. In the initial work Collins et al. used a two-component system consisting of $[Zr(Cp)_2(Me)(thf)][BPh_4]$ and $[Zr(Cp)_2(Me)_2]$ for the synthesis of PMMA.[1] The product obtained showed the same tacticity as PMMA obtained in nonstereospecific polymerizations. Later it was reported that the cationic enolate complex $[Zr(Cp)_2\{OC(OMe)=C(Me)_2\}(thf)][BPh_4]$ initiates the polymerization of MMA with very low efficiency.[2]

In the same time Soga et al. showed that the reaction of dimethylzirconocenes with $[Ph_3C][B(C_6F_5)_4]$ or $B(C_6F_5)_3$ yields cationic zirconcenes that can be activated for polymerization of MMA with alkyl zinc and alkyl aluminum coumpounds.[3] Both research groups showed that multicomponent catalytic systems containing bridged dimethylzirconocenes yield isotactic PMMA. Only recently Collins et al. reported on the bridged Cp−amidozirconocene $[Zr\{(C_5Me_4)(t\text{BuN})Me_2Si\}\{OC(OR)=CMe_2\}(L)]$ (L = THF, O=C(OR)CHMe$_2$) which polymerizes MMA at low temperatures to isotactic PMMA.[4] Related work using samarocene catalysts was reported by Yasuda et al.[5]

Recently we showed, for the first time, that $[Zr\{(Cp)(Ind)CMe_2\}(Me)(thf)][BPh_4]$ is a stereospecific, highly active one-component catalyst for the synthesis of isotactic PMMA,[6] a result which was later confirmed by others.[7] We postulated the mechanism of this reaction by correlating experimental results with the results of ab initio calculations.[8] We also showed that $[Zr\{(Cp)_2CMe_2\}(Me)(thf)][BPh_4]$ yields syndiotactic PMMA with high efficiency.[9] However, we found $[Zr(Cp)_2(Me)(thf)][BPh_4]$ to be inactive, and $[Zr\{(Cp)_2SiMe_2\}(Me)(thf)][BPh_4]$ weakly active. The initial steps of acrylate polymerizations were calculated by Sustmann et al. using simplified zirconocene complexes as catalysts and acrylic acid as a model substrate.[10] According to this work three different mechanisms should be possible, each of which involving a different active species: a cationic, a neutral and/or a bimetallic one. Since $[Zr(Cp)_2(Me)(thf)][BPh_4]$ and $[Zr\{(Cp)_2CMe_2\}(Me)(thf)][BPh_4]$ are inactive and active, respectively, we felt the need to add more theoretical work in order to better understand the initial reaction steps and thus undertook calculations on our catalyst systems, the results of which are reported here.

Computational Details

All calculations were carried out using the Gaussian98 program package.[11a] Geometry optimizations and energy calculations were done on the B3LYP level of theory. As basis sets we used the 6-31G* basis set as is implemented in the Gaussian98 program package for C, H, and O. For Zr we used the DZVP basis set by Godbout et al.[11b] This combination we denote as basis set 1 (B1). Some model complexes, which are mentioned explicitly in the text, have been optimized on the B3LYP/3-21G level of theory. Before starting the study we checked the quality of the B3LYP/B1 method by comparing calculated structures of known compounds with their corresponding crystal structures[11c,d] and found the theoretical method to yield satisfying results. For some compounds, which are explicitly mentioned in the text, solvent effects were included by calculations of single point energies using the CPCM solvation model (COSMO) as is implemented in Gaussian98.[11e−g]

All geometries were checked by frequency calculations to prove successfully if they were minima (zero imaginary frequencies) or saddle points of order one for transition states (one imaginary frequency). All opti-

* Corresponding author. Fax: (+49) 241-8022185. E-mail: hoecker@dwi.rwth-aachen.de.

10.1021/ma020413f CCC: $22.00
Published on Web 09/11/2002

Table 1. Energies *E* (hartree) and Zero Point Corrected Energies E_{ZPE} (hartree) of Compounds Calculated in This Work on the B3LYP/B1 Level[a]

compd	*E*	E_{ZPE}	compd	*E*	E_{ZPE}
1b	−4084.1786	−4083.9104	**1u**	−3967.4497	−3967.2458
2b	−4316.6821	−4316.3038	**2u**	−4199.9608	−4199.6362
3b	−4430.0318	−4429.6376	**3u**	−4313.3006	−4312.9698
4b	−4430.0343	−4429.6360	**4u**	−4313.2962	−4312.9617
5b	−4662.4778	−4661.9631	**5u**		
6b	−4662.4909	−4661.9756	**6u**	−4545.7547	−4545.3032
7b	−4775.8138	−4775.2938	**7u**	−4659.0786	−4658.6216
8b	−4775.8265	−4775.3055	**8u**	−4659.0891	−4658.6318
11b	−4775.8644	−4775.3412	**11u**	−4659.1304	−4658.6709
12b	−5121.6475	−5120.9982	**12u**		
15b	−4775.8751	−4775.3482	**15u**	−4659.1416	−4658.6779
16b	−5121.6698	−5121.0169	**16u**	−5004.9373	−5004.3479
17b	−4775.8536	−4775.3281	**17u**	−4659.1103	−4658.6498
18b	−5121.6792	−5121.0235	**18u**	−5004.9425	−5004.3492
TS3b-4b	−4429.9991	−4429.6029	**TS3u-4u**	−4313.2621	−4313.9291
TS8b-17b	−4775.7636	−4775.2425	**TS8u-17u**		
TS11b-15b	−4775.8495	−4775.3257	**TS11u-15u**	−4659.1139	−4658.6533
TS16b-18b	−5121.6515	−5120.9980	**TS16u-18u**	−5004.9113	−5004.3215
3Si	−4681.4580	−4681.0731			
4Si	−4681.4573	−4681.0685			
TS3Si-4Si	−4681.4231	−4681.0364			
MMA	−345.7865	−345.6625			
THF	−232.4494	−232.3321			

[a] Basis set B1, see computational details.

Table 2. Energies *E* (hartree) of 3, 4, and TS3-4 Obtained on the B3LYP/B1 Geometries Including Solvent Effects[a]

compd	*E*	ΔE [b]
3b	−4430.0822	
TS3b-4b	−4430.0506	+19.83
4b	−4430.0853	−1.94
3u	−4313.3537	
TS3u-4u	−4313.3168	+23.15
4u	−4313.3511	+1.63

[a] Calculated using the CPCM solvation model using dichloromethane as solvent. [b] Relative to reactant (kcal/mol).

mized transition states were used as input for IRC calculations to successfully prove that the transition state indeed connects the corresponding reactants and products. All geometry optimizations were carried out with no constraints. For the discussion in the text we use the energies as obtained (in kcal/mol, Table 1), and ZPE-corrected energies are also provided in Table 1 (energies of solvated compounds are listed in Table 2).

Results and Discussion

In a cationic mechanism, as was calculated before,[10] the addition of acrylic acid to the zirconocene enolate complex $[Zr(Cp)_2\{-O-C(OH)=CH_2\}]^+$ (**A**) is an exothermic reaction yielding **B** (Scheme 1). Also the formation of a C−C single bond between coordinated acrylic acid and the $CH_2=C(OH)O-$ fragment (via transition state **C**), yielding the eight-membered metallacycle **D** is exothermic. Only the final step, the dissociation of the coordinated C=O group of **D** yielding **E** is strongly endothermic, rendering this mechanism unfavorable. The authors also stated, that addition of another molecule of acrylic acid to **B** results in the formation of **F**, which is an exothermic process again, and also **F** reacts to yield **G** in an exothermic reaction. The dissociation of the C=O group of **G**—leading to **H**—is slightly endothermic or slightly exothermic, depending on the computational method used. A neutral and a bimetallic mechanism were also discussed. Since our catalytic reactions start with dichloromethane solutions of complexes $[Zr(Cp)_2(Me)(thf)][BPh_4]$ and $[Zr\{(Cp)_2CMe_2\}(Me)(thf)][BPh_4]$, with MMA being present in a large excess and with the weakly coordinating BPh_4 anion, we considered (i) the cationic mechanism to be the active one and (ii) the formation of the C−C single bond between the enolate and the acrylic acid in the model system (i.e, reaction **B** to **D** in Scheme 1) not to be crucial for the start of the catalytic cycle, since the reacting carbon atoms are too far away from the zirconocene fragment to be influenced significantly. To understand why $[Zr\{(Cp)_2CMe_2\}(Me)(thf)][BPh_4]$ is a highly active catalyst whereas $[Zr(Cp)_2(Me)(thf)][BPh_4]$ is not, we thought that the different reaction behavior arises from the methyl transfer step, which would be necessary if a cationic mechanism were operative. Since we postulated before that a 5-fold coordinated zirconium center was necessary to enable a stereoselective reaction

Scheme 1. Energy Profile for the Initial Steps of Acrylic Acid Polymerization after Sustmann et al.[10] [a]

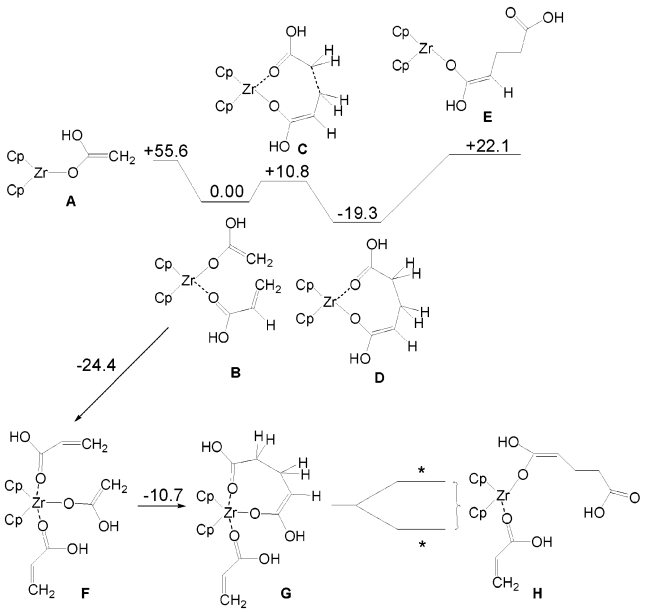

[a] Energies in kcal/mol; details cf. text; * = depending on computational method.

using [Zr{(Cp)(Ind)CMe_2}(Me)(thf)][BPh_4] as catalyst, we investigated also if a 5-fold coordinated zirconium center is involved in the methyl transfer step.

Alternative Reaction Pathways. All calculated molecules are schematically depicted in Scheme 2 (see legend for Scheme 2) and the structures of all calculated compounds are shown in Figure 1. We refer to all bridged compounds as ***n*b** and to all unbridged compounds as ***n*u**.

Compound **1** was calculated for completeness and to monitor the huge energy release upon adding the oxygen donors THF and MMA to it (**2**, **3**). Which are the reactions cation **2** can undergo? The exchange of the THF molecule in **2** by MMA yields complex **3** (Scheme 2). Alternatively **2** might add one MMA molecule without losing the THF molecule. In this way compounds **5** and **6** are created. In **5** the methyl group is moved toward the THF molecule, resulting in a position in the middle between the THF and the MMA molecule. In **6** the positions of MMA and the methyl group are exchanged. Analogously, also **3** might add another MMA molecule leading to complexes **7** and **8**. Furthermore, **3** might undergo the methyl transfer directly. We elucidate the different reactions paths, starting with **3**.

Assuming that **3** reacts directly, the methyl group is transferred to the MMA molecule which results in the formation of the ester enolate **4** in which the oxygen and the C−C double bond of the enolate unit coordinate to the zirconium center, with one of the hydrogen atoms of the transferred methyl group weakly completing the metal's coordination sphere (Scheme 2, Figure 1). The reaction of **3b** to **4b** is exothermic by −1.57 kcal/mol, whereas interestingly **4u** is by +2.76 kcal/mol richer in energy than **3u** (discussion of activation energies vide infra). When MMA is added to **4** yielding **11** −28.92 and −27.17 kcal/mol of energy are liberated for **11b** and **11u**, respectively. The reaction of **11** to **12** is not possible. The transformation of **11b** to **12b** is endothermic by +2.13 kcal/mol, whereas all attempts to optimize **12u** resulted in the formation of **11u** and one MMA molecule which moved away completely from the complex. Thus, **11** reacts to **15** at first, resulting in compounds **15b** and **15u**, which are more stable by −6.71 and −7.03 kcal/mol respectively, than the corresponding reactants **11b** and **11u**. From here on, the reaction proceeds via addition of a new MMA molecule, thus yielding **16b** and **16u**, which are lower in energy by −5.14 and −4.20 kcal/mol, respectively. Then the next C−C bond is formed, and the resulting products are **18b** and **18u**, being more stable by −5.90 and −3.26 kcal/mol than **16b** and **16u**, respectively.

Alternatively, **3** might take up another MMA molecule yielding **7** and **8**. In **7** the methyl group resides in the middle between the two coordinated MMA molecules, while in **8** the central ligand position is occupied by MMA. Both **7b** and **7u** are clearly endothermic products by +2.82 and +5.33 kcal/mol with respect to their reactants **3b** and **3u**, respectively. Furthermore, complex **9** could not be located, although we tried several starting geometries. Thus, we did not consider the reaction path **3** → **7** → **9** further. However, the reaction to **8** is exothermic. **8b** and **8u** are more stable by −5.14 and −1.26 kcal/mol than their reactants. The reaction of **8** to **11** should either proceed via compound **10** or **17**. However, several attempts to locate stationary points on the hypersurface for **10** were unsuccessful for both **10b** and **10u**. In all cases we only obtained **11**. For **17** the situation is different, since both **17b** and **17u** could be located. **17b** is more stable than **8b** by −17.00 kcal/mol, and upon forming **17u** from **8u**, −13.30 kcal/mol is liberated. Instead of obtaining **11** only via the sequence **3** → **4** → **11** the sequence **3** → **8** → **17** → **11** now also has to be considered. These two sequences will be inspected more closely (vide infra).

Turning back to **2** there are two more possible products, i.e., **5** and **6**. Compound **5b** was located, and it is weakly endothermic (+0.50 kcal/mol) relative to **2b**. Complex **5u** was not located, although we have tried several starting geometries: The THF molecule is always expelled from **5u** yielding isolated **3u** and THF. Since **5b** is slightly endothermic and since energetically more favorable reaction paths are available, we consider the path **2** → **5** → **13** not to be operative. However, **2** can also react to **6**, which is a clearly exothermic reaction for both **6b** and **6u**, liberating −7.72 and −4.64 kcal/mol, respectively. So we searched for the structure of **14**. But as before with **10**, it was not possible to locate the product **14**. We used several starting geometries for both **14b** and **14u** but were not able to locate minimum structures in which the methyl group is transferred though still being coordinated via one of its hydrogen atoms. Instead, in all products, the methyl group and the carbon chain to which it is bound are rotated away from the metallocene fragment, leading to a sole coordination of the enolate oxygen and the oxygen atom of the THF molecule to the zirconium center.

Alternatively it can be envisioned that **6** reacts analogously to **8**, i.e., to form a product like **17**, since the presence of a THF molecule compared to a MMA molecule as in **8** should not create a noticeable difference—and the THF molecule would have to be replaced by MMA anyway later on; otherwise, this reaction sequence would not be operative. For this reason, it is sufficient to elucidate the reaction steps evolving from **8**.

Without having considered activation energies at this point, the possible reaction pathways are as follows: **2** → **3** → **4** → **11** → **15** → **16** → **18** and **2** → **3** → **8** → **17** → **11** → **15** → **16** → **18**.

Activation Energies and Solvent Effects. To obtain the activation energies of the two sequences mentioned, we calculated the structure of the transition states **TS3b-4b** and **TS3u-4u** and found their energies to be higher by +20.52 and +24.16 kcal/mol relative to the energies of the reactants **3b** and **3u**, respectively. The activation energy of the unbridged compound is higher, and we consider this as the reason for the inactivity of this molecule in the temperature range used experimentally (−30 to +30 °C[9]): the reaction of **3b** to **4b** is approximately 400 times faster than the reaction of **3u** to **4u**.[12a] However, the energies of the transition states differ not so much as to easily rule out solvent effects, which can decrease the energetics of molecular systems quite substantially. Thus, we recalculated the energies of the series **3**, **TS3-4**, and **4** by performing self-consistent reaction field single point calculations on the B3LYP/B1 geometries using the CPCM solvation model.[11e−g] These results are summarized in Table 2. As expected the energies of all compounds in this series are lowered (**TS3b-4b** +19.83 kcal/mol, **TS3u-4u** +23.15 kcal/mol), though not overly and—most important—the trend observed for the gas-phase calculations is confirmed.[12b]

Further confirmation is provided by the reaction of [Zr{$(Cp)_2SiMe_2$}(Me)(thf)][BPh_4]. This compound is ac-

Scheme 2. Alternative Reaction Pathways for the Initial Steps of MMA Polymerization Using Bridged and Unbridged Zirconocenes and Energies on the B3LYP/B1 Level of Theory (Only Bridged Compounds Are Shown)[a]

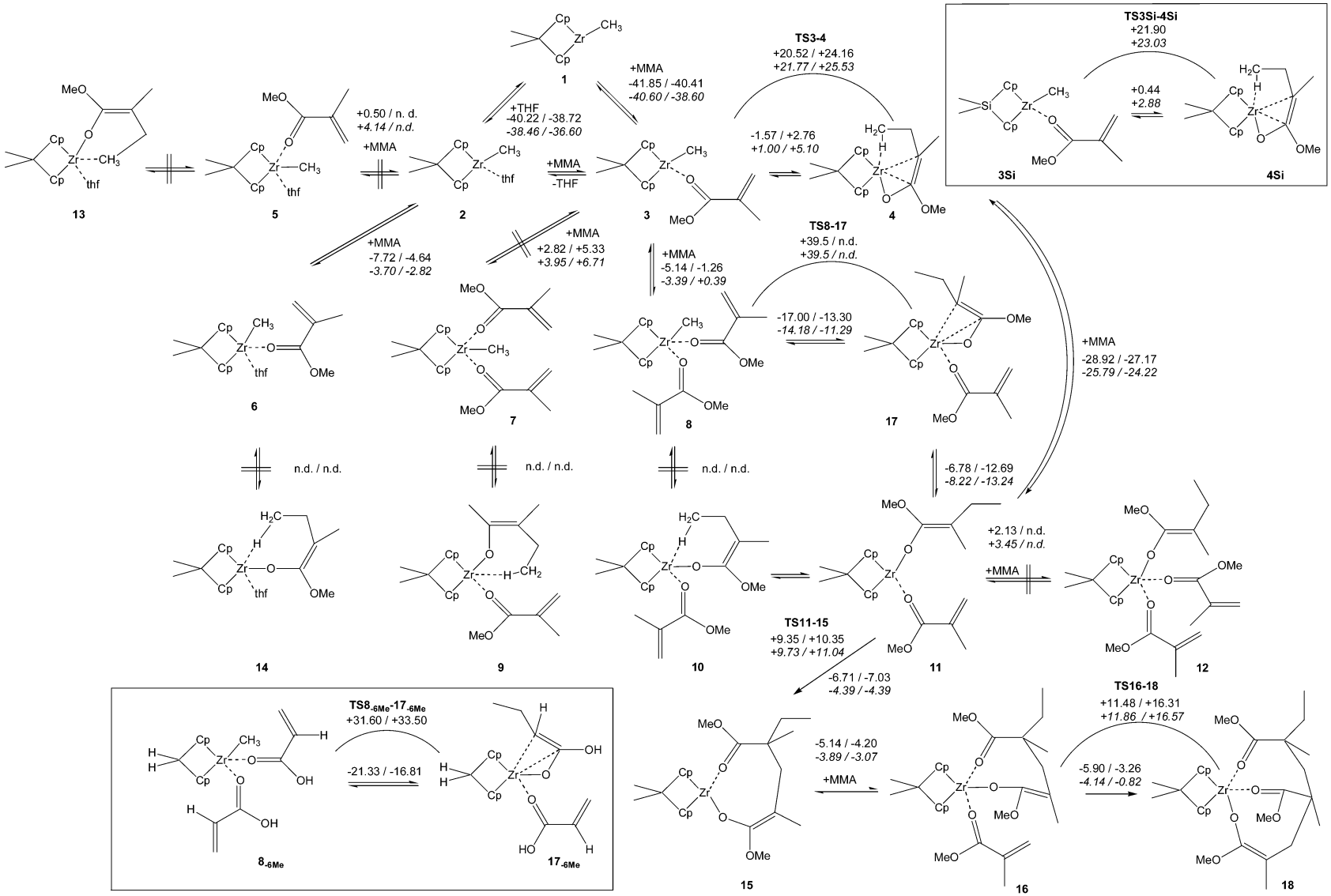

[a] Figures close to or above reaction arrows are energy differences $E = E_{product} - E_{reactant}$ of bridged/unbridged zirconocenes ***n*b**/***n*u** [kcal/mol] (the ZPE corrected energy differences are given in italics). Figures over a bow give the energy of the corresponding transition state—designated as TS*n*-*m*—for the particular reaction relative to the energy of the reactant. n.d. = not determined (details see text). The insert in the upper right shows the energy profile of the methyl transfer in Me_2Si-bridged zirconocenes, and the insert in the lower left shows the energy profile of the methyl transfer using the 6-fold demethylated model complexes **8**$_{-6Me}$ → **17**$_{-6Me}$ (calculations on these model compounds were carried out on the B3LYP/3-21G level of theory; see also ref 14).

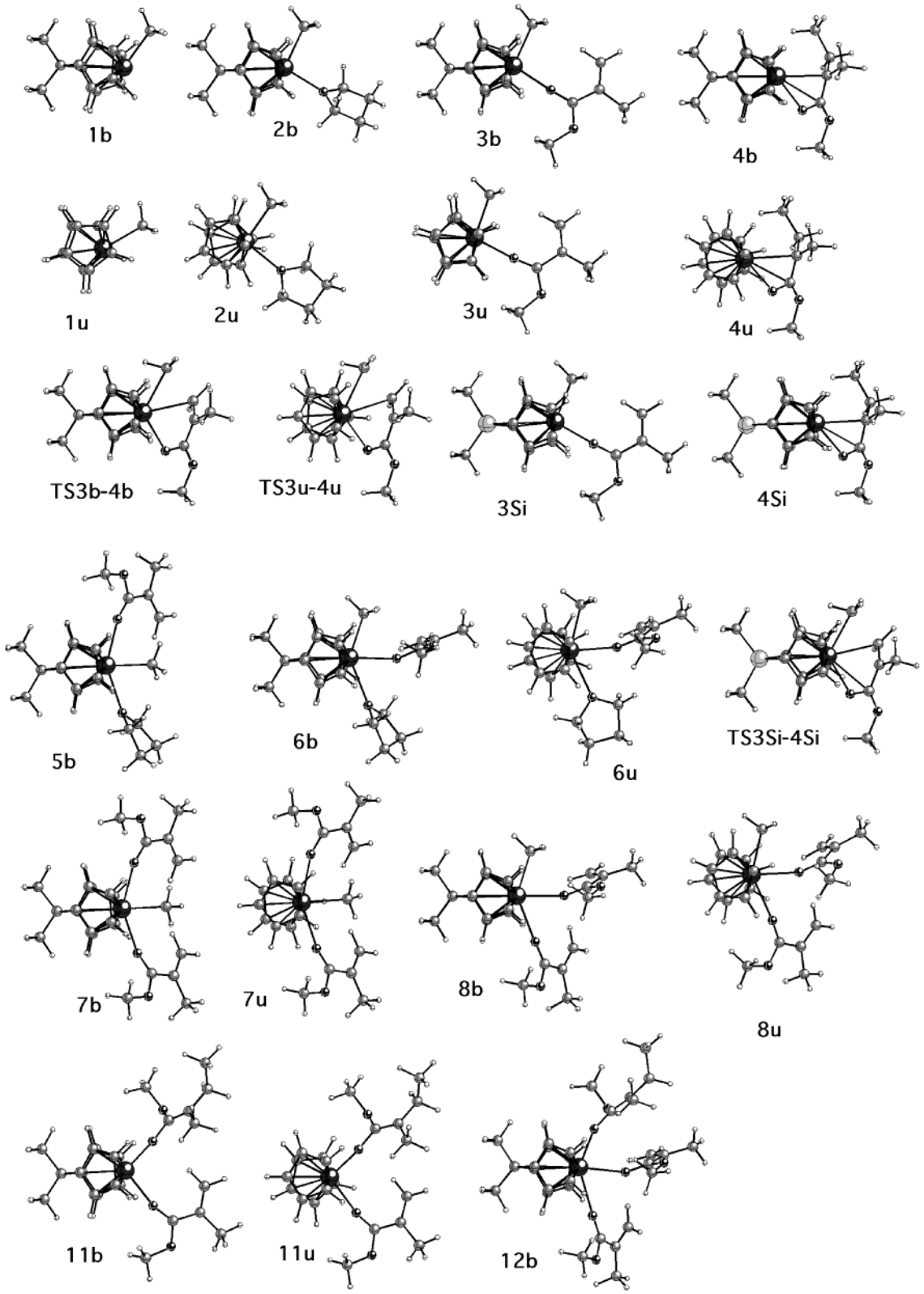

tive; however, the turnover numbers are significantly lower compared to those for [Zr{$(Cp)_2CMe_2$}(Me)(thf)][BPh_4]. According to the calculated energies of Me_2Si-bridged **3** and **4** (**3Si**, **4Si**), the product **4Si** is richer in energy by +0.44 kcal/mol relative to **3Si** (see upper insert in Scheme 2). The energy of the transition state **TS3Si-4Si** is by +21.90 kcal/mol above the energy of **3Si** and thus lies between the energies of **TS3b-4b** and **TS3u-4u**. It is noteworthy that the relative order of stability of all products **4** and—more important—of all transition states **TS3-4** is in accordance with the reaction behavior of the true catalysts.

In the sequence **8** → **17** the picture is a little different. Here both **17b** and **17u** are clearly exothermic products relative to **8b** and **8u**. However, the energy of the transition state **TS8b-17b** is higher than the reactant's energy by +39.5 kcal/mol. This activation energy is too high for the reaction to proceed via **8b** → **17b**.[12]

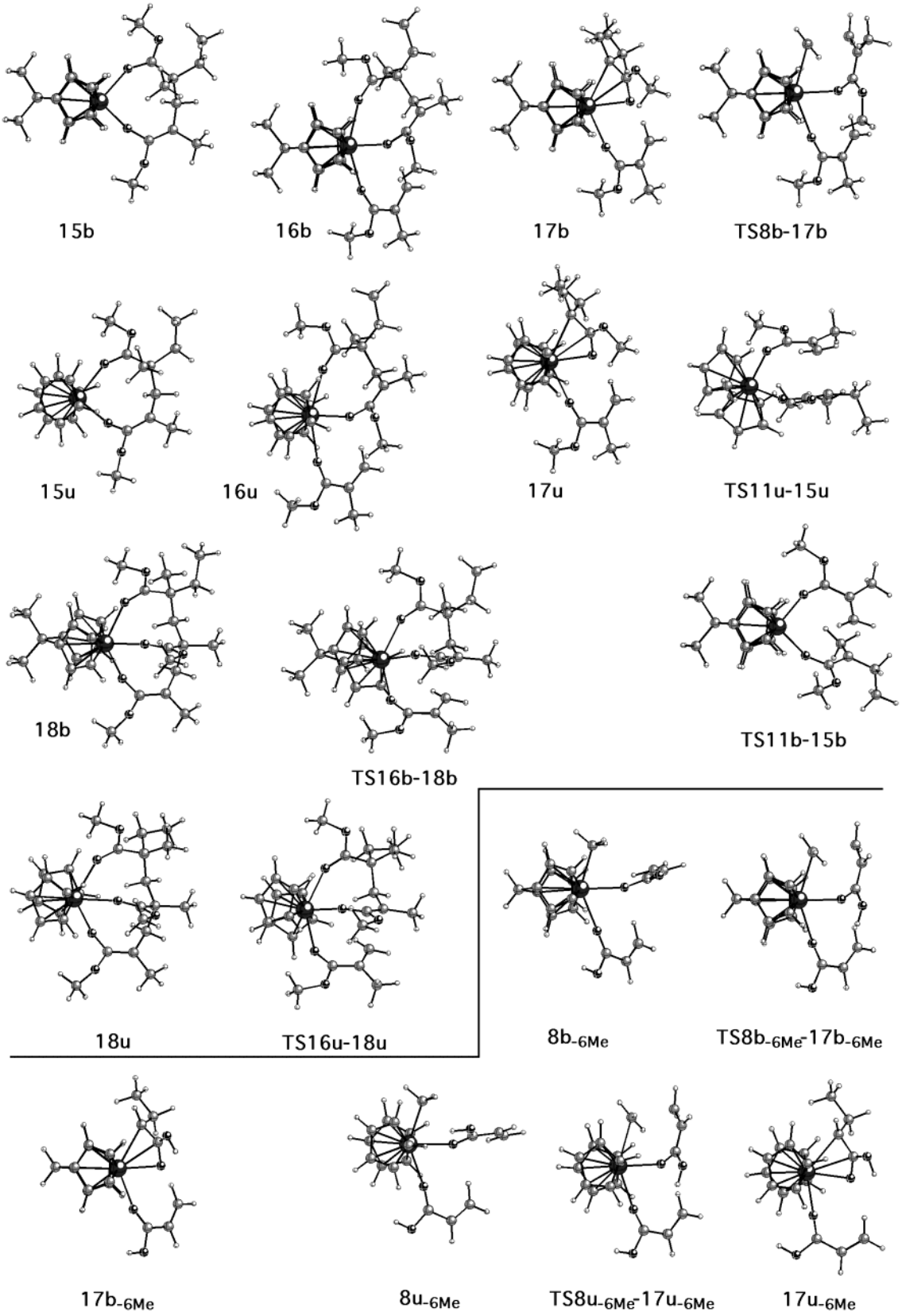

Figure 1. Ball and stick representation of the structures of all calculated compounds shown in Scheme 2 (elements in decreasing size: Zr, Si, C, O, H).

Interestingly, **17u** cannot be formed starting from **8u**, since we were not able to locate the transition state for this reaction. Many attempts to find **TS8u-17u** resulted in the formation of transition states of **11u** (in which the rotations of methyl groups were the only result of the search of the transition state).[13] As a result **17b** will not be formed from **8b**, because the activation energy is too high and **17u** will neither be formed from **8u**, since the transition state is not existing (see also ref 13 and the lower insert in Scheme 2).

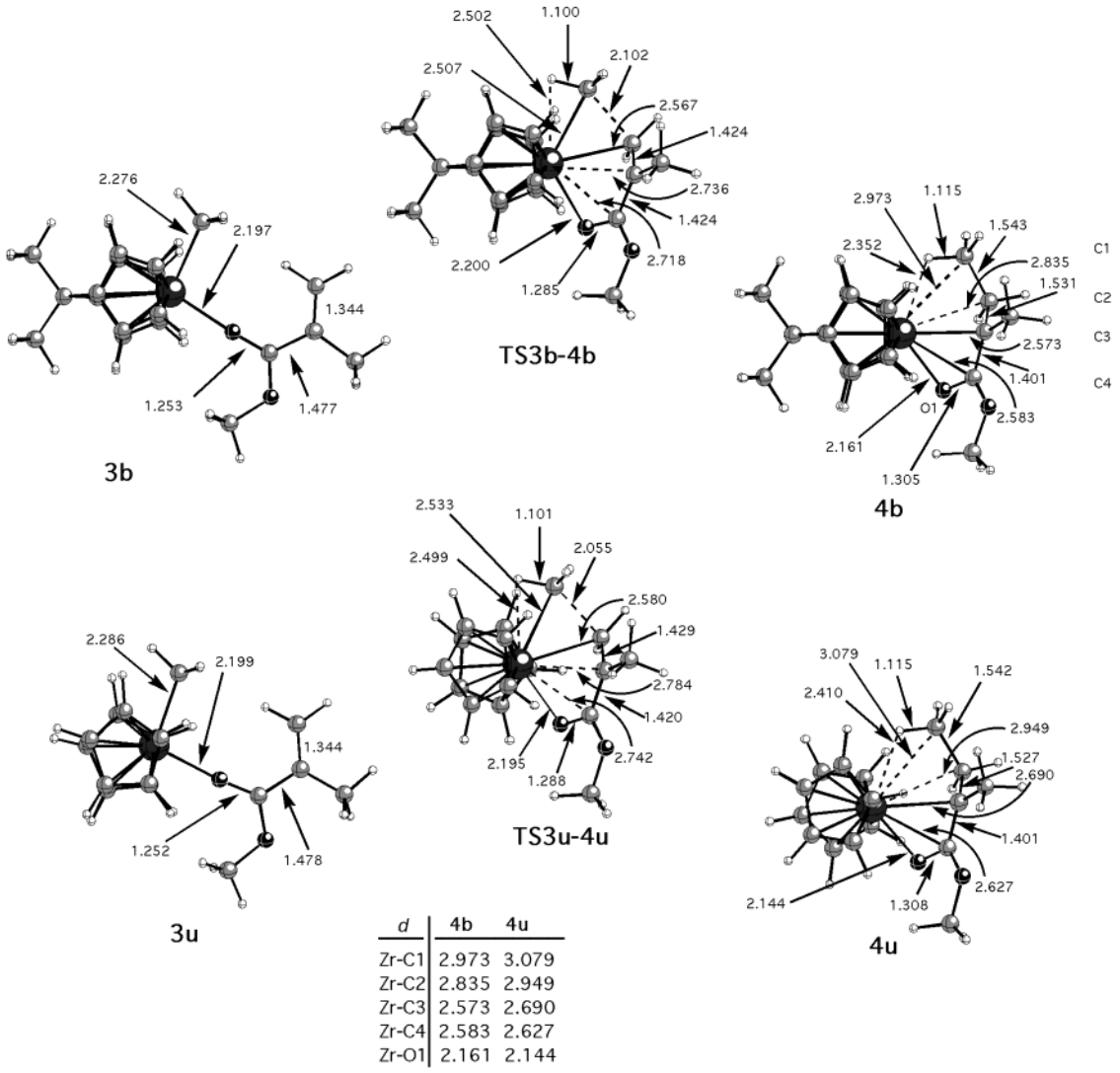

d	4b	4u
Zr-C1	2.973	3.079
Zr-C2	2.835	2.949
Zr-C3	2.573	2.690
Zr-C4	2.583	2.627
Zr-O1	2.161	2.144

Figure 2. Ball and stick representation with selected atom distances (Å) of **3**, **4**, and **TS3-4**.

Consequently the reaction does only proceed via the sequence **3** → **4,** which is predicted to be more difficult for **3u** than for **3b**. Thus, the unbridged catalyst is incative, in accordance with our experimental results.

Upon reaction of **11** to **15**, the first C−C bond is formed between the ester enolate moiety and the coordinated MMA molecule. The energies of the transition states are considerably lower compared to the ones in the methyl transfer step and amount to +9.35 and +10.35 kcal/mol for **TS11b-15b** and **TS11u-15u**, respectively, indicating that this reaction is not only possible but also not influenced by the geometry of the metallocene. As we assumed before, the similarity in energies for the two transition states is a clear indication that the metallocene fragment does not influence the energetics of the C−C bond formation. As we have shown earlier,[8] the carbonyl oxygen atom does not dissociate from the Zr center to create a vacant coordination site for the next MMA molecule; instead, the whole eight-membered ring moves to one side and in this way creates a vacant coordination site for MMA (**16**). The reaction from **16** to **18** proceeds via transition states **TS16b-18b** and **TS16u-18u** which are higher in energy by +11.48 and +16.31 kcal/mol relative to the reactants, respectively.

Structural Features of 4b and 4u. A closer inspection of the structural parameters of **4b** and **4u**—which are summarized in Figure 2—made clear that (i) the bond lengths and angles are practically equal within the enolate moieties of the two compounds, (ii) that in **4u** the atoms of the enolate unit are significantly further away from the zirconium center compared to **4b**, (iii) that the zirconium center in **4b** is located further away from/outside the Cp region, and (iv) that the larger distance between the enolate moiety and the zirconium center in **4u** compared to **4b** is most probably responsible for weaker attractive interactions in **4u**; i.e., there is no energy gain by transferring the methyl group, and the attractive interactions between enolate and zirconium center are substantially weaker in **4u**. In other words, the zirconium center is better accessible in **4b** than in **4u**. This is reflected by the enolate−zirconium distance: The enolate moiety is bent away from the zirconocene fragment in the order **4b**, **4Si**, and **4u**, with the Zr−O distance remaining nearly unchanged (see table included in Figure 2; values for **4Si** not shown graphically). The Cp−Zr−Cp angle which varies significantly from 115.2° (**4b**) over 124.0° (**4Si**) to 127.5°-(**4u**) indicates the same trend: The Cp orbitals overlap better with the ones of the zirconium center in **4u**, compared to **4Si** and **4b**. The enolate moieties in **4b** and **4u**, being partly delocalized systems, should generally interact in a better way with the zirconocene than a single bonded methyl group and a MMA molecule

coordinated by its carbonyl oxygen (**3b** and **3u**), however only if the overlap is strong enough, which is not the case in **4u**. Furthermore, the relative orientation of the Cp rings to each other in **4u** might also play a role: The partly staggered conformation of the Cp rings in **4u** leads to shorter distances between the hydrogen atoms of the Cp ring and the hydrogen atoms of the methyl group of the former MMA in **4u** (atom distances ca. 2.35 and 2.68 Å). In **4b**, the eclipsed conformation of the Cp rings causes larger distances between hydrogen atoms of the Cp ring and hydrogen atoms of the methyl group (d_{min} = 2.90 Å). In other words, energetically it will be relatively more unfavorable to push the enolate unit in **4u** closer to the zirconium center because (i) the electron demand of the zirconium center is not pronounced enough to benefit from this and (ii) repulsive interactions between hydrogen atoms of the Cp rings and hydrogen atoms at C1 will be of a more pronounced strength.

Conclusions

The study presented herein provides theoretical clarification for the different reaction behavior of [Zr{$(Cp)_2CMe_2$}(Me)(thf)][BPh_4] and [$Zr(Cp)_2$(Me)(thf)][BPh_4] in the polymerization of MMA. It was shown that the crucial step for the reaction is the methyl transfer step which is energetically favorable for the reaction of **3b** to **4b** due to the corresponding low activation energy. For the reaction of **3u** to **4u** it is too high, which is the reason why [$Zr(Cp)_2$(Me)(thf)][BPh_4] is inactive in MMA polymerization. A participation of 5-fold coordinated zirconium complexes in the methyl transfer was considered to be less likely, since the obtained products are either endothermic (**5b**, **7b**, **7u**) or do not exist (**5u**). In cases where complexes with 5-fold coordinated zirconium centers are exothermic (**6b**, **6u**, **8b**, **8u**), we were unable to locate the following reaction products (**10**, **14**), which means that **6** and **8** would have to react directly to yield **11**. However, a direct transfer of the methyl group in **8** and **6** to yield **11** (and a product like **11**, respectively, in which the MMA unit is replaced by THF) is most improbable, since a complete cleavage of the Zr−Me bond would be necessary without compensating for the increased eletron demand of the zirconium center by other organic moieties present in these complexes. An alternative reaction path from **8** to **11** via **17** is not possible due to the high energy of the transition state **TS8-17** (as was confirmed by calculations on model complexes). Furthermore, the energies of all other transition states (**TS3-4**, **TS11-15**, and **TS16-18**) are low enough for the reaction to proceed.

Acknowledgment. This work was supported by the Bundesministerium für Forschung und Technologie (BMBF, No. 03C0276B/O). We are grateful for a generous allocation of computer time by the Hochschulrechenzentrum, RWTH Aachen, and thank A. Lorenz for technical assistance. For helpful discussions we are grateful to Prof. Dr. G. Frenking (Marburg).

References and Notes

(1) Collins, S.; Ward, D. G. *J. Am. Chem. Soc.* **1992**, *114*, 5460−5462.

(2) Collins, S.; Ward, D. G.; Suddaby, K. H. *Macromolecules* **1994**, *27*, 7222−7224.

(3) (a) Soga, K.; Deng, H.; Shiono, T. *Macromolecules* **1994**, *27*, 7938−7940. (b) Soga, K.; Deng, H.; Shiono, T. *Macromolecules* **1995**, *28*, 3067−3073. (c) Soga, K.; Deng, H.; Shiono, T. *Macromol. Chem. Phys.* **1995**, *196*, 1971. (d) Soga, K.; Saito, T.; Saegusa, N.; Hagihara, H.; Ikeda, T.; Deng, H. *Macromol. Chem. Phys.* **1998**, *199*, 1573−1579.

(4) Nguyen, H.; Jarvis, A. P.; Lesley, M. J. G.; Taylor, N. J.; Collins, S. *Macromolecules* **2000**, *33*, 1508−1520.

(5) (a) Yasuda, H.; Yamamoto, H.; Yokota, K.; Miyake, S.; Nakamura, A. *J. Am. Chem. Soc.* **1992**, *114*, 4908−4910. (b) Yasuda, H.; Furo, M.; Yamamoto, H.; Nakamura, S.; Miyake, N.; Kibino, N. *Macromolecules* **1992**, *25*, 5, 5115−5116. (c) Yasuda, H.; Yamamoto, H.; Takemoto, Y.; Yamashita, M.; Yokota, K.; Miyake, N.; Nakamuara, A. *Makromol. Chem., Macromol. Symp.* **1993**, *67*, 187. (d) Yasuda, H.; Yamamoto, H.; Yamashita, M.; Yokota, K.; Nakamuara, A.; Miyake, S.; Kai, Y.; Kanehisa, N. *Macromolecules* **1993**, *26*, 7134−7143. (e) Yasuda, H.; Ihara, E. *Macromol. Chem. Phys.* **1995**, *196*, 2417−2441.

(6) Stuhldreier, T.; Keul, H.; Höcker, H. *Macromol. Rapid Commun.* **2000**, *21*, 1093−1098.

(7) (a) Cameron, P. A.; Gibson, V. C.; Graham, A. J. *Macromolecules* **2000**, *33*, 4329−4335. (b) Erker, G. Personal communication.

(8) Hölscher, M.; Keul, H.; Höcker, H. *Chem.—Eur. J.* **2001**, *7*, 5419−5426.

(9) Frauenrath, H.; Keul, H.; Höcker, H. *Macromolecules* **2001**, *34*, 14−19.

(10) Sustmann, R.; Sicking, W.; Bandermann, F.; Ferenz, M. *Macromolecules* **1999**, *32*, 4204−4213.

(11) (a) Gaussian 98, Revision A.11, Gaussian, Inc., Pittsburgh, PA, 1998. (b) Godbout, N.; Salahub, D. R.; Andzelm, J.; Wimmer, E. *Can. J. Chem.* **1992**, *70*, 560. (c) Thewalt, U.; Guthner, T. *J. Organomet. Chem.* **1989**, *59*, 379 (CCDC-code: SEHMOH) (d) Jordan, R. F.; Bajgur, S. C.; Willett, R.; Scott, B. *J. Am. Chem. Soc.* **1986**, *108*, 7410−7411 (CCDC code: FAGLAA). (e) Klamt, A.; Schürmann, G.; *J. Chem. Soc., Perkin Trans. 2* **1993**, 799. (f) Andzelm, J.; Klömel, C.; Klamt, A.; *J. Chem. Phys.* **1995**, *103*, 9812. (g) Barone, V.; Cossi, M.; *J. Phys. Chem.* **1998**, *A 102*, 1995.

(12) (a) As a rough estimation of how the obtained activation energies are related to the rate of the reaction we used the Arrhenius equation: $k = Ae^{(-Ea)/(RT)}$. With frequency factors of 10^9 and 10^{14} s^{-1} (values like this are common for many reactions both in the gaseous and in the liquid phase) and a temperature of 300 K we obtained k values of 1.1×10^{-6} and 0.11 s^{-1} respectively, when an activation energy of 20.52 kcal/mol (85.91 kJ/mol; transformation of **3b** to **4b**) is used. Assuming that the rate constant k for this step represents one turnover, there are ca. 0.004 and 400 turnovers/h, respectively. Regarding the reation of **3u** to **4u** the activation energy is 24.16 kcal/mol (+101.06 kJ/mol), which leads to k values of 2.5×10^{-9} and 2.5×10^{-4} s^{-1} (which represent 9×10^{-6} and 0.9 turnovers/h, respectively). This means that the reaction of the bridged system is roughly 400 times faster than the one of the unbridged system. However, when the activation energy is ca. 40 kcal/mol (167 kJ/mol), as in the tranformation of **8b** to **17b**, with the frequency factors and the temperature being the same, then the turnovers/h are 3.0×10^{-17} and 3.0×10^{-12}, respectively. Concluding from the activation energies, they are low enough for **3b** to react to **4b** in short reaction times, and the transformation **3u** → **4u** is too slow to produce polymer in reasonable times. Furthermore **8b** will not react to form **17b**; (b) We would like to bring clearly to the readers' attention that systems of this kind might contain more complexity than was elucidated so far by experiments and calculations: one reviewer pointed out to us that the calculated activation barriers seem to oppose the experimentally derived activation energy for initiation for the bridged system as was reported in ref 9. However, this observation is most probably an artifact, since in ref 9 we reported only on the experimentally derived activation energies for the catalyst containing the Me_2C(Cp)-(Ind) ligand. It might be argued that the Me_2C(Cp)(Ind) ligand behaves electronically exactly the same as the Me_2C-$(Cp)_2$ ligand (which we have not investigated), and thus we note that experimental and theoretical results stand as is and should stimulate further investigations (the reader might want to take into consideration that our laboratory techniques do not allow for a precise monitoring of a truly representative amount of datapoints for the very first seconds of the reaction − one possible reason, why the experimental results might contain a substantially larger error than was estimated in ref 9).

(13) We are aware of the fact that not having located **TS8u-17u** does not necessarily mean that it does not exist. It might have

been overseen since the hypersurface is complex and subtle differences in the starting geometry of the transition state (i.e., in the position on the hypersurface) might well be the reason for this. However, even if it were overlooked, it can easily be imagined that the energy of the transition state has to have a value similar to that of **TS8b-17b**, since the MMA molecule needs to be rotated and bent in the same way. Also the methyl group would have to be moved into the same direction by approximately the same amount. For this reason, we consider the reaction from **8u** to **17u** to be as unfavorable as the one from **8b** to **17b** (vide supra). To support this assumption, we performed the same calculations on the B3LYP/3-21G level of theory using model complexes $\mathbf{8}_{-6Me}$ and $\mathbf{17}_{-6Me}$ in which six of the seven methyl groups of **8** and **17** were replaced by hydrogen atoms (see lower inset in Scheme 2). As expected the energy profiles are similar to the ones of the reaction **8** → **17**. Upon forming $\mathbf{17b}_{-6Me}$ out of $\mathbf{8b}_{-6Me}$, −21.33 kcal/mol is released (−16.81 kcal/mol for the unbridged system) and the transition state $\mathbf{TS8b}_{-6Me}$-$\mathbf{17b}_{-6Me}$ is by +31.60 kcal/mol richer in energy than the corresponding reactant. The energy of the unbridged transition state $\mathbf{TS8u}_{-6Me}$-$\mathbf{17u}_{-6Me}$ is somewhat higher (+33.50 kcal/mol), which in turn confirms our assumption: The activation energies for the sequence **8** → **17** are too high for the reaction to proceed.

MA020413F